

# Ambiguity Function Side-Lobes Reduction in WiFi-Based Passive Bistatic Radar

Fabiola Colone, Paolo Falcone, Pierfrancesco Lombardo, Tullio Bucciarelli

*INFOCOM Dept., University of Rome "La Sapienza",  
via Eudossiana 18 - 00184 Rome, Italy*

**Abstract**—In this paper the feasibility of a WiFi transmissions based passive bistatic radar is analysed. The auto-correlation function of this waveform of opportunity is characterized with reference to typical signals broadcasted by a 802.11 access point. The obtained auto-correlation function is shown to yield a high sidelobe level which strongly limits the useful dynamic range. These sidelobe structures have a deterministic nature mainly related to the exploited modulation and coding schemes. Proper weighting networks are proposed to cope with this limitations based on the knowledge of the expected value of signal autocorrelation function. The performance of the proposed technique is evaluated against simulated data generated according to the 802.11 Standards. Moreover the preliminary results are presented against a real data set collected by an experimental setup. The proposed approach is shown to yield a significant improvement of the peak to sidelobe ratio thus making the considered waveform more attractive for PBR local area surveillance.

## I. INTRODUCTION

In recent years the use of Passive Bistatic Radar (PBR) for surveillance purposes has received renewed interest, e.g. [1]. PBR exploits existing illuminators of opportunity to perform target detection which results in the exciting possibility of low cost surveillance, reduced pollution of the Electro-Magnetic environment, etc.

PBR operation does inherently imply that the transmitted waveform is not within the control of the radar designer. As a consequence the corresponding ambiguity function may show sidelobes at a level not greatly lower than that of the peak which can lead to target echoes being masked by disturbance contributions in the received signal (direct signal breakthrough and multipath reflections), thus strongly limiting the detection capability of the system.

Among all the emitters available in the environment, broadcast transmitters represent some of the most attractive choices for long surveillance applications, owing to their excellent coverage. Specifically the most common signals for PBRs in use today are non-cooperative frequency modulated (FM) commercial radio stations since they offer a good trade off between performance and overall system development costs, [2]. A number of studies have looked at the use of different analogue signals such as HF radio and UHF television broadcasts, [3]-[4], as well as digital transmissions

such as DAB, DVB and GSM, [5]-[6]. In the above applications, PBR is rapidly reaching a point of maturity. Basically, even though there are still many challenges to be solved involving both technology development and processing techniques, PBR practical feasibility for long range surveillance purposes has been well established.

In this paper we investigate the possibility of new PBR applications with reference to local area monitoring. Aiming at the detection and localization of designated human beings or man-made objects within short ranges, wider bandwidth signals of opportunity should be exploited to achieve the required range resolution. To this purpose wireless local area network transmissions might be considered, [7]. Wireless networking applications are proliferating at a very rapid rate for both commercial and private use. One of the most popular systems consists of the IEEE 802.11 Standards based (WiFi) technology, [8], which offers reasonable bandwidth (range resolution) and coverage and a wide accessibility.

These transmissions sources might potentially act as an ideal illuminator of opportunity for short range detection and surveillance using the PBR principle. However WiFi transmissions are complex, a number of standards have been developed and further versions are being investigated. The three most commonly being deployed are 802.11a, 802.11b and 802.11g. According to the physical layer specifications adopted by each standard, in typical operation modes, a WiFi access point may be broadcasting a mix of signals based on different modulations and coding schemes, which strongly affect the corresponding autocorrelation function. However, an 802.11 access point periodically transmits a regular Beacon signal broadcasting its presence and channel information. The Beacon signal uses a combination of direct sequence spread spectrum / differential binary phase shift keying (DSSS/DBPSK) and DSSS / differential quadrature phase shift keying (DSSS/DQPSK) based on a 11-chip Barker sequence.

In this paper the auto-correlation function of the Beacon signal is characterized. Specifically we show that the detection performance of a WiFi Beacon signal-based PBR can be strongly limited by the ambiguity properties of the exploited signal. In fact the target returns are likely to be masked by the high level sidelobes resulting from the disturbance contributions even in the presence of a significant range-

Doppler separation. However, for the considered transmissions, based on digital modulation schemes, these sidelobes have a deterministic behaviour and can be significantly reduced almost if an exact knowledge of their shape is available. Thus, based on this approach, an effective processing technique is presented in this paper to minimize the masking effects of the disturbance contributions resulting from the Beacon signal range sidelobes. The performance of the proposed approach is analysed with reference to both simulated and real data sets. Specifically the feasibility of a WiFi-based PBR is preliminary demonstrated using an experimental setup developed and fielded at the InfoCom Dept. of the University of Rome “La Sapienza”.

The paper is organized as follow. The Beacon signal modulation and coding schemes are described in Section II where the resulting auto-correlation function is evaluated. In Section III an ad hoc weighting network is presented for the suppression of the Barker code sidelobes while a proper filter for the reduction of additional sidelobes structures is proposed in Section IV. Section V reports the description of the experimental setup and the results obtained against the collected data sets by jointly applying the proposed techniques in a practical PBR scenario. Finally our conclusion are drawn in Section VI.

## II. BEACON SIGNAL AUTO-CORRELATION FUNCTION (ACF)

A number of 802.11 standards have been developed and further versions are being investigated. The three most commonly being deployed are 802.11a, 802.11b and 802.11g. 802.11a is only adopted in the Regulation Domain of the United States and operates in the 5 GHz band while 802.11g represents the third generation of this wireless networking standards after 802.11 and 802.11b and maintains a full compatibility with the older standards operating in the 2.4 GHz band. These standards allow different data rates and operate according to different frequency channels plans. The different data rates are achieved by exploiting different modulations and coding schemes according to the physical layer (PHY) specifications adopted by each standard. The main modulations are either DSSS or orthogonal frequency-division multiplexing (OFDM) and data rates between 1 and 54 Mbps are currently specified. Notice that DSSS is the most common modulation with OFDM dominating only at higher data rates.

As previously mentioned, an 802.11 access point usually broadcasts a great variety of signals based on different modulations and coding schemes. However it periodically transmits a regular Beacon signal broadcasting its presence and channel information.

The Beacon signal exploits a DSSS modulation using baseband modulations of DBPSK and DQPSK. The DSSS system provides a processing gain of at least 10 dB which is accomplished by chipping the baseband signal at 11 MHz with an 11-chip PN code. The following 11-chip Barker

sequence is used as the PN code sequence

$$\mathbf{c} = [1, -1, 1, 1, -1, 1, 1, 1, -1, -1, -1] \quad (1)$$

where the leftmost chip is output first in time. The first chip is aligned at the start of a transmitted symbol so that each symbol duration is exactly 11 chips long. Thus a DSSS frame of N transmitted symbols can be written as:

$$s_{DSSS}(t) = \sum_{n=0}^{N-1} d_n b(t - nT_s) \quad (2)$$

where  $d_n$  is the  $n$ -th complex symbol according to the particular modulation scheme (BPSK, QPSK),  $T_s=1 \mu\text{s}$  is the symbol duration and  $b(t)$  is the symbol pulse shape:

$$b(t) = \sum_{k=0}^{10} c[k] w(t - kT_c) \quad (3)$$

being  $c[k]$  the  $k$ -th element in the 11-chip Barker sequence given in (1) and  $w(t)$  the chip time-window of duration  $T_c=T_s/11=0.0909 \mu\text{s}$ .

The transmitted frame for each Beacon signal is composed by the Preamble, the Header field and the Payload (see Figure 1). The preamble contains the following fields: SYNC (a sequence of 128 scrambled ones) and SFD (a fixed 16-bit field). The header field (48 bit) contains information about the payload (length, data rate, modulation, etc.), finally the payload contains the beacon frame (which is a MAC level frame). The preamble and header fields are based on a DBPSK modulation (1 Mbps, 192  $\mu\text{s}$ ), while the payload uses DQPSK modulation (2 Mbps).

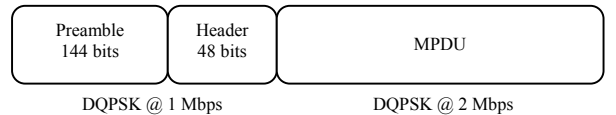


Figure 1 – The Beacon Frame structure

A software tool has been developed for Beacon frame simulation according to the above description with random generation of the payload bits. Using the simulated signals, the corresponding auto-correlation function (ACF) can be evaluated as:

$$\chi(\tau) = \int_{-\infty}^{+\infty} s_{DSSS}(t) s_{DSSS}^*(t + \tau) dt \quad (4)$$

This represents the output of the Beacon signal matched filter. As an example, the ACF obtained for a Beacon frame of about 0.4 ms of duration is reported in Figure 2 (blue curve).

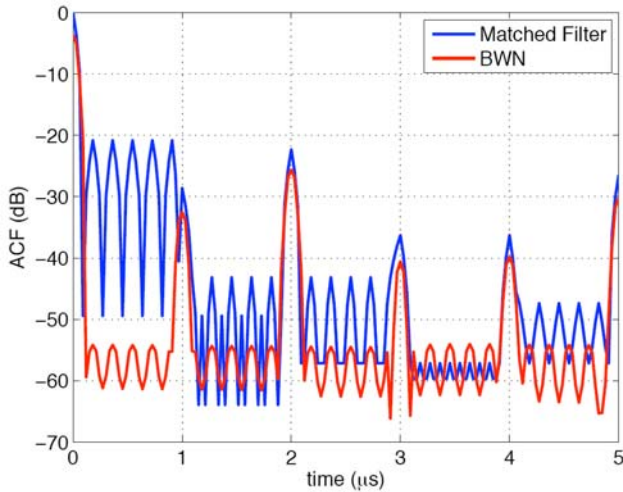


Figure 2 – ACFs for a simulated WiFi Beacon Frame of duration 0.4 ms

As it is apparent, strong sidelobe structures appear in the ACF which might be responsible for significant masking effects if such waveform is used for PBR target detection. Notice that, aiming at a local area surveillance application, a delay extent of 5  $\mu$ s has been considered which corresponds to a range extent of 1.5 km.

Specifically, five almost identical sidelobes appear within time delays of 1  $\mu$ s (300 m) which are obviously due to the exploited 11-chip Barker code. As expected, these sidelobes show a peak to sidelobe ratio (PSR) of  $20\log_{10}(11) = 20.83$  dB and a temporal separation equal to  $2T_c$ . In addition, other strong sidelobes appear at delays multiple of  $T_s$  ( $k=300$  m). This sidelobe structures are due to the cyclical repetition of the Barker code and their level equals the average correlation among consecutive symbols of the Beacon frame.

In the hypothesis of statistical independence between consecutive transmitted symbols and assuming ergodicity, it can be shown that the level of these periodic sidelobes would dramatically decrease when very long frames are considered. However they cannot be neglected if Beacon frames of limited duration are exploited as available in the considered pulsed transmissions.

Notice that the described characteristics of the Beacon signal ACF are only dependent on the exploited modulation and coding schemes so that they also apply to other DSSS signals broadcasted by a WiFi access point with data rates of 1 Mbps and 2 Mbps.

Thus, in the following, proper filters are presented for the sidelobes level control distinguishing between those deriving from the Barker code and those appearing at multiples of  $T_s$ .

### III. WEIGHTING NETWORK FOR BARKER SIDELOBES REDUCTION

Aiming at reducing the Barker sidelobes in the Beacon signal ACF, we exploit the weighting network proposed in [9]. Using the discrete time version of (4), the ACF of the 11-

chip Barker code in (3) is given by:

$$\chi_b[n] = \sum_{k=0}^{10} b[k]b[k+n] \quad (5)$$

where  $b[k]$  are the samples of signal  $b(t)$  at time instants  $tk=kT_c$  and

$$\chi_b[n] = \begin{cases} 0 & n \text{ odd} \\ 11 & n = 0 \\ -1 & n \text{ even} \end{cases} \quad (6)$$

The design of the weighting network for sidelobe reduction of the Barker code (Barker weighting network, BWN) exploits the above description of its ACF. Aiming at implementing the BWN as a transversal filter, its impulse response can be written as:

$$h_{BWN}[k] = \sum_{n=-M}^M \alpha_n \delta[k-n] \quad (7)$$

where the total filter length is given by  $2M+1$ . Thus the output of this weighting network applied to the Barker code ACF is given by:

$$\begin{aligned} z[k] &= \chi_b[k] * h_{BWN}[k] = \\ &= \sum_{n=-10}^{10} \sum_{i=-M}^M \chi_b[n] \alpha_i \delta[k-(n+i)] \end{aligned} \quad (8)$$

The peak value is obtained at index  $k=0$  while the sidelobes region occupies indices  $\pm k$  with  $k = 1, 2, \dots, M+10$ . Thus the statements of the optimization problem are:

$$\begin{aligned} z[0] &= \sum_{n=-10}^{10} \chi_b[n] \alpha_n = \max \\ |z[k]| &= \left| \sum_{n=-10}^{10} \chi_b[n] \alpha_{k-n} \right| \leq 1 \end{aligned} \quad (9)$$

Each modulus inequality of the system in (9) is substituted by two linear inequalities, and the problem is solved using well-known linear programming algorithms. As an example, Figure 3 shows the BWN coefficients obtained for  $M=12$  (filter length  $2M+1=25$ ). As it is apparent, the filter is symmetrical and has non-zero values only at even indices. It is easy to show that this is a general result whatever is the filter length. Thus the block diagram of the BWN is that shown in Figure 4. Obviously the cascade of the matched filter and the BWN can be replaced by a single “mismatched” filter of proper length.

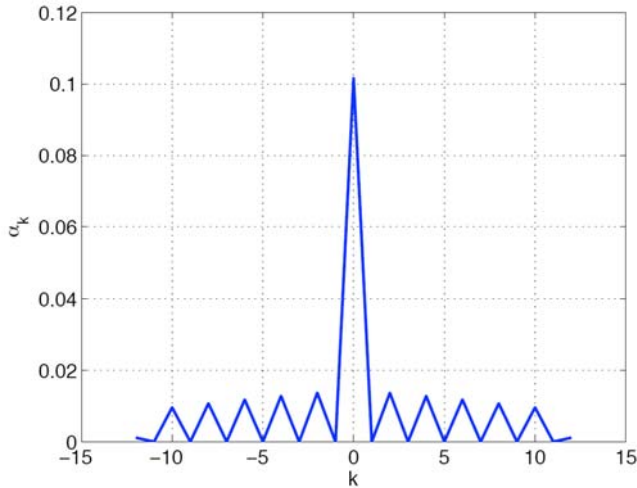


Figure 3 – Barker Weighting Network coefficients for  $M = 12$  BWN

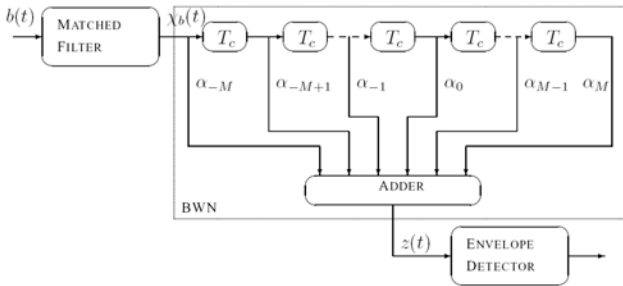


Figure 4 – Sketch of the Barker Weighting Network

Obviously, by properly selecting the filter length, different values of the PSR can be achieved as reported in Table I.

TABLE I:  
PEAK TO SIDELOBE RATIO FOR DIFFERENT BWN LENGTHS

M	Filter Length	PSR (dB)
12	25	26.5
25	51	34
50	101	50
75	151	63

The result of the application of BWN with total length  $2M+1=101$  is reported in Figure 2 (red line) compared to the result of the matched filter case (blue line). As expected the BWN dramatically decrease ACF sidelobes due to the Barker code so that a PSR equal to about 50 dB is obtained within time delays of  $0.8 \mu\text{s}$ . Notice that, based on the application requirements which set the filter length, the filter weights evaluation has to be performed only once. However, the conceived weighting network is ineffective against the periodic sidelobe structure due to the non-zero correlation among consecutive symbols of the Beacon frame. A proper strategy to counteract this effect is presented in the next Section.

#### IV. ADDITIONAL SIDELOBES REDUCTION

Aiming at the detection of targets at delays higher than  $0.8 \mu\text{s}$  (ranges higher than 240m), the ACF sidelobes at multiples of  $1 \mu\text{s}$  should be reduced to avoid masking effects on targets appearing at those delays. To this purpose the estimate of the ACF values at  $tk=kT_s$  can be exploited to design an effective sidelobe reduction filter. Indicating with  $\chi(kT_s)$  the ACF samples at delays multiple of  $T_s$ , the required reduction of these periodical sidelobes can be obtained by subtracting from the original ACF properly scaled and delayed replicas:

$$\chi_r(\tau) = \chi(\tau) - \sum_{\substack{k=-K \\ k \neq 0}}^K \gamma_k \chi(\tau - kT_s) \quad (10)$$

where  $K$  is the number of range sidelobes to be removed on both sides of the ACF main peak and  $\gamma_k$  is the scaling factor for the  $k$ -th sidelobe and is given by:

$$\gamma_k = \frac{\chi(kT_s)}{\chi(0)} \quad (11)$$

Thus the transfer function of this additional sidelobes reduction filter (ASRF) is given by:

$$H_{ASRF}(f) = 1 - \sum_{\substack{k=-K \\ k \neq 0}}^K \gamma_k \exp(-j2\pi f k T_s) \quad (12)$$

The number  $K$  of sidelobes to be reduced can be arbitrarily selected aiming at removing periodical sidelobes contribution over a given range extent corresponding to the surveillance area. As an example Figure 5 shows the resulting ACF obtained after the application of the ASRF with  $K=4$  (black line). The matched filter output is also reported in Figure 5 for comparison (blue line).

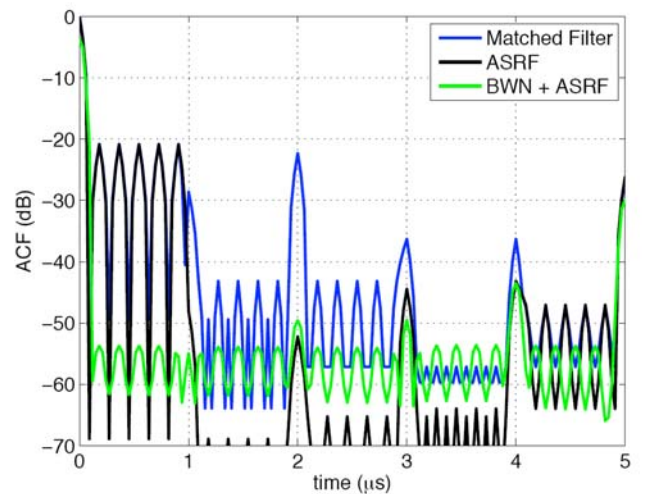


Figure 5 – ACFs for a simulated WiFi Beacon of duration 0.4 ms

In contrast to the results obtained with the BWN, the ASRF is able to strongly reduce the sidelobes at delays multiples of  $T_s$  while keeping almost unchanged those related to the Barker code. Specifically a PSR higher than 40 dB is obtained for delay values between 1  $\mu$ s and 4.8  $\mu$ s corresponding to ranges within the interval [300 m, 1260 m].

Notice that the ASRF can be applied after the BWN by properly modifying the scaling factors, namely the samples of the BWN-filtered ACF should be used. The ACF resulting from the cascade of the two different sidelobe reduction filters is shown in Figure 5 (green line). Notice that a PSR value greater than 40 dB is obtained for ranges smaller than 1260 m with only a small power loss which is mainly due to the BWN.

## V. EXPERIMENTAL RESULTS

In this section the results obtained against a real data set are reported. Specifically the experimental setup is described in subsection V.A and the autocorrelation function analysis is presented in subsection V.B thus demonstrating the effectiveness of the proposed techniques against real signals. Finally the feasibility of the WiFi-based PBR is demonstrated in subsection V.C with reference to its detection performance in a practical scenario.

### A. Experimental Setup

The experimental setup is sketched in Figure 6. As it is well known, in PBR systems, the transmitted waveform is not available at the receiver as in conventional monostatic systems and therefore a dedicated and separate receiver channel is required to collect the transmitted signal. This is subsequently used as the reference signal and is correlated with the surveillance channel signal for target echo detection.

To this purpose, a portable wireless access point (D-Link DAP 1160) is connected to the transmitting antenna while a -20dB fraction of the transmitted signal is gathered in a dedicated receiving channel (reference channel) by using a directional coupler which yields a 0.5dB insertion loss and isolation greater than 20dB. The second channel of a dual-channel receiving system was directly connected to a separate receive antenna which was used to collect the surveillance signal. The antennas are characterized by a beamwidth of about 15° and a front to back ratio greater than 30dB.

The receiving system uses a single fully coherent down conversion stage for the two channels, so as to move the central frequency of the selected WiFi channel to an intermediate frequency of 15 MHz. After adequate filtering and amplification, the signal is sampled with a sampling frequency equal to 55 MHz using a high quality dual channel A/D converter with a wide dynamic range (software selectable), controlled by an external stable and tunable oscillator.



Figure 6. Sketch of the Experimental setup.

The acquired IF data was stored and processed off-line using digital filters. Specifically the following stages were implemented:

- transmitted pulses automatic detection;
- modulated signal complex envelope extraction (digital down-conversion – DDC).

Different tests were performed in a low clutter outdoor environment (a parking area in Cisterna di Latina, Italy, see Figure 7) using vehicular targets.

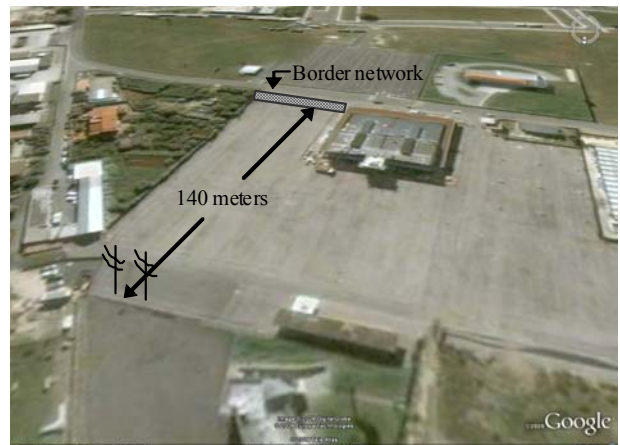


Figure 7. WiFi experiment area in Cisterna di Latina

For the target detection experiment considered in the following, the wireless access point was configured to transmit in channel 7 of the WiFi band (centre frequency of 2.437 GHz), which is a portion of industrial, scientific and medical (ISM) frequency band. It was set up to roam for connected devices emitting the beacon signal at 1 ms intervals. A quasi-monostatic configuration was adopted for the two antennas which were mounted one on top of the other. Two targets were present (a car and a motorbike) moving backward and forward, respectively, in the parking area at approximately 30 km/h. In this case an acquisition of duration of about 4 sec. is available consisting of approximately 2,000 Beacons.

### B. Autocorrelation Analysis

Firstly the signal collected at the reference channel has been used to evaluate the autocorrelation function of the considered signal of opportunity and to test the proposed sidelobes reducing techniques.

Figure 8 shows the reference signal ACF (output of the matched filter, blue line), the output of the BWN (red line) and the output of the ASRF (green line). The reported curves have been estimated over a limited portion of the available file (10 consecutive Beacons). As expected, the ACF shows the typical structure of the Barker sidelobes with only small deviations due to the access point and the receiving channel filters which reduce the actual signal bandwidth with respect to its nominal value. As a direct consequence of these deviations, the BWN is not able to obtain the theoretical peak to sidelobes ratio of 50 dB. However notice that a PSR greater than 35 dB is obtained which results in a significant increase of the useful dynamic range. Finally, notice that the ASRF is able to strongly reduce the first 4 lobes due to the correlation among the symbols of the Beacon frame. The reported results clearly show the effectiveness of the proposed techniques against real data. In the following subsection their benefits will be demonstrated with reference to the target detection issue.

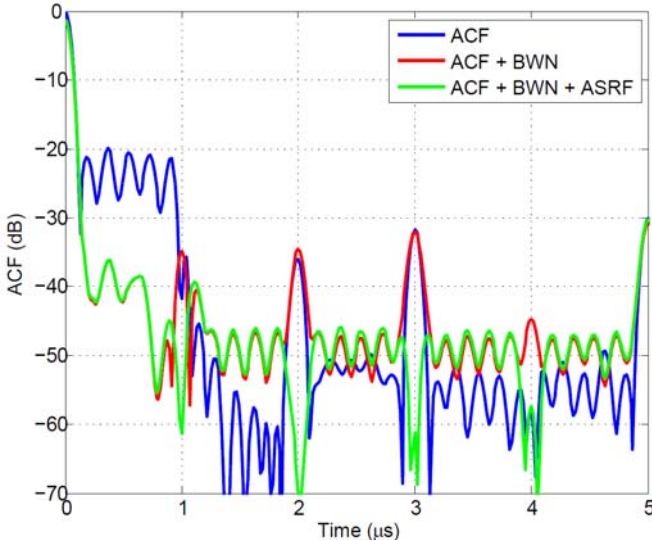


Figure 7. Reference signal ACF and corresponding filtered versions.

### C. Target Detection Test

The target detection performance of the WiFi-based PBR system has been analysed with reference to the experimental test previously described. A 2D (delay-Doppler) cross-correlation function (2D-CCF) is evaluated by cross-correlating the surveillance signal with Doppler-shifted replicas of the reference signal:

$$\chi[l, p] = \left| \sum_{i=0}^{N_{int}-1} s_{surv}[i] \cdot s_{ref}^*[i-l] \cdot e^{-j2\pi pl / N_{int}} \right| \quad (13)$$

where

- $l=0, \dots, R-1$  is the time bin representing the time delay  $\tau[l]=lT_s$ , being  $T_s=1/f_s$  the sampling period; the time delay can be converted in a bistatic range difference by defining the corresponding range bin as  $\Delta R[l] = c \cdot \tau[l]$ ; using a monostatic geometry the range becomes simply  $\Delta R[l] = c \cdot \tau[l]/2$ ;
- $p$  is the Doppler bin representing the Doppler frequency  $f_D[p]=p/(N_{int}T_s)$ , being  $N_{int}$  the number of integrated samples, namely the number of samples on which the 2D-CCF is estimated; a Doppler measurement  $f_d$  might be univocally related to a bistatic velocity  $v$  ( $f_d=v/\lambda$ , where  $\lambda$  is the wavelength corresponding to the carrier frequency  $f_c$  and  $v=v_{Tx}+v_{Rx}$  being  $v_{Tx}$  and  $v_{Rx}$  the target relative velocities with respect to the Tx and the Rx); thus in the monostatic case we have  $f_d=2v_{Tx/Rx}/\lambda$ .

Figure 8(a) shows the 2D-CCF evaluated over an integration period of 1 sec. which allows a Doppler resolution equal to 1 Hz (velocity resolution equal to 0.22 km/h) thus yielding a much better target localisation over the range-velocity plane. As it is apparent, a strong peak appears at range 15 m and zero velocity corresponding to the direct signal transmitted by the transmitting antenna and collected by the sidelobes of the receive antenna. The temporal delay of the direct signal is due to the length of the cables (being each cable about 15 meters long). Another strong peak appears at range 155 m and zero velocity due to the reflection of the transmitted signal over the border network (see Figure 7).

Due to the pulsed nature of the considered signal of opportunity the impulse response of the matched filter in the Doppler dimension shows severe sidelobes structure which cannot be removed by using a conventional weighting network. In fact these sidelobes represent Doppler ambiguities due to the non regular Beacon transmitting frequency. Notice that, even configuring the access point to transmit the beacon signal at 1 ms intervals, we experienced a variable Beacon repetition period due to the capability of the WiFi system to “sniff” the shared medium before starting transmission.

The interaction between the Doppler and the range sidelobes due to the Barker code yields a quite high sidelobe level all over the 2D-CCF which completely masks the two targets returns.

Figure 8(b) reports the output of the cascade of the matched filter, the Barker weighting network and the Additional Sidelobes Reduction Filter. As it is apparent, the sidelobe level has been significantly reduced so that two isolated peaks now appear at locations corresponding to the distances and velocities of the considered targets. Notice that in our specific case the application of the ASRF is not strictly necessary since the maximum range searched for detection is limited by the border network which acts as an electromagnetic shield.

Obviously, when only interested in the detection of moving targets, the complete removal of the returns at zero velocity might be obtained using a proper adaptive cancellation filter along the line suggested in [10], which however requires an

additional computational load. Even in this case, the application of the proposed techniques still yields a significant advantage by counteracting the masking effect of strong target returns over weaker ones.

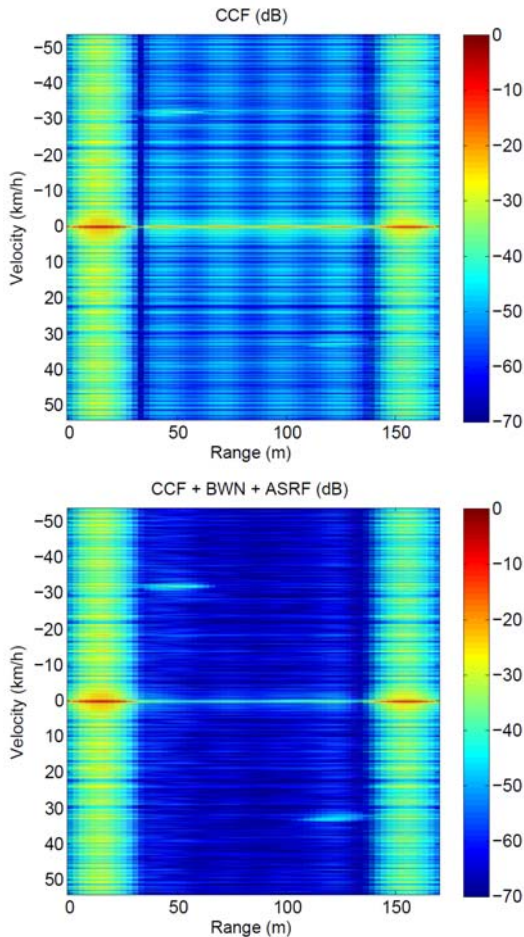


Figure 8. CCFs for the surveillance signal using: (a) the original reference signal (matched filter); (b) the BWN/ASRF-filtered version of the reference signal

## VI. CONCLUSIONS

In this paper the ambiguity characteristics of the Beacon signals broadcasted by a 802.11 access point have been analysed.

Aiming at exploiting such waveform of opportunity for PBR purpose, an effective weighting network has been presented to reduce the range sidelobes due to the particular modulation and coding schemes adopted. The proposed network shows a very limited complexity and can be implemented using a transversal filter structure operating with a limited number of taps. It has been shown to yield really improved PSR values with respect to the application of a standard matched filter. Specifically PSR greater than 40dB can be obtained, with respect to the 20dB of the original ACF, which significantly increases the useful dynamic range for PBR surveillance application. The effectiveness of the

proposed techniques has been verified against real WiFi signals in practical scenarios by preliminary demonstrating the feasibility of a WiFi-based PBR in vehicular targets monitoring application.

Obviously such an application would require improved target localization capability. Notice that much better target localization can be obtained using Doppler if a suitable integration time is used; however the integration time needs to be traded off against the computational load and the expected target migration. The range resolution is obviously limited by the signal bandwidth (11 MHz for DSSS WiFi transmissions) and thus would appear to be more suitable for a longer range outdoor application. In this regard, a significant improvement is expected for the longer range and wider bandwidth WiMAX (IEEE 802.16) system. Moreover the use of further localisation methods such as multiple receivers and triangulation is expected to be able to further improve the effective range resolution of a WiFi-based passive radar system. This might also enable the use of this technique in a number of applications including tracking of moving objects, people or vehicles in indoor and outdoor environments.

## REFERENCES

- [1] S. I. on Passive Radar Systems, *IEE Proceedings on Radar, Sonar and Navigation*, vol. 152, Issue 3, pp. 106–223, June 2005.
- [2] P. Howland, D. Maksimiuk, and G. Reitsma, “FM radio based bistatic radar,” *IEE Proceedings on Radar, Sonar and Navigation*, vol. 152, Issue 3, pp. 107–115, June 2005.
- [3] H. Griffiths and N. Long, “Television based bistatic radar,” *IEE Proc. F, Commun. Radar Signal Process*, vol. 152, Issue 3, pp. 649–657, June 1986, 133, (7).
- [4] G. Fabrizio, F. Colone, P. Lombardo, and A. Farina, “Adaptive beamforming for high frequency over-the-orizon passive radar,” *in printing on IET Proc. on Radar, Sonar and Navigation*.
- [5] C. Coleman and H. Yardley, “Passive bistatic radar based on target illuminations by digital audio broadcasting,” *IET Radar, Sonar and Navigation*, vol. 2, Issue 5, Oct. 2008.
- [6] R. Saini and M. Cherniakov, “DVT signal ambiguity function analysis for radar application,” *IET Proc. on Radar, Sonar and Navigation*, vol. 152, no 3, pp. 133–142, June 2005.
- [7] H. Guo, K. Woodbridge, and C. Baker, “Evaluation of WiFi beacon transmission for wireless based passive radar,” *Department of Electronic and Electrical Engineering, University College London Torrington Place, WC1E 7JE, London, UK*.
- [8] *Wireless LAN Medium Access Control (MAC) and physical Layer (PHY) Specification*, IEEE Std. 802.11, 2007.
- [9] R. Bilocchi, T. Bucciarelli, and P. T. Melacci, “Radar sensitivity and resolution in presence of range sidelobe reducing networks designed using linear programming,” *The Radio and Electronic Engineer*, vol. 54, pp. 224–250, June 1984.
- [10] F. Colone, D.W. O’Hagan, P. Lombardo, C. J. Baker, “A multistage processing algorithm for disturbance removal and target detection in Passive Bistatic Radar”